14th IEA Heat Pump Conference
15-18 May 2023, Chicago, Illinois

Performance Analysis of High-Temperature Heat Pumps with Two-Phase Ejectors

Pengtao Wang, Stephen Kowalski, Cheng-Min Yang, Jian Sun, Zhiming Gao, Kashif Nawaz*

Multifunctional Equipment Integration Group, Building Technology Research and Integration Center, Oak Ridge National Laboratory, Oak Ridge, TN 37831, USA

* Corresponding author. Tel.: +1-865-241-0972.
E-mail address: nawazk@ornl.gov.

Abstract

A two-phase ejector recovers the energy in the refrigerant cycles' throttling process, improving the coefficient of performance (COP) of high-temperature heat pumps (HTHPs). This study investigated the effects of the mixing pressure on the performance of two-phase ejectors and ejector-assisted HTHPs. A 1D theoretical model of a two-phase ejector was built to predict the internal fluid dynamics and evaluate ejector performance. A thermodynamic model of an ejector-assisted HTHP was built to evaluate the COP of HTHPs and the volumetric heating capacity of low-global warming potential refrigerants. The results demonstrate that an optimum mixing pressure in a two-phase ejector provides the best performance of a two-phase ejector and ejector-assisted HTHP. The optimum mixing pressure was slightly lower than the evaporation pressure. At this pressure, the two-phase flow in the ejector was subsonic. For ejector-assisted HTHPs using low–global warming potential refrigerants at a sink temperature of 120°C, temperature lift of 40°C, and subcooling of 10°C, a two-phase ejector has an average ejector efficiency of 0.334, and the COP and volumetric heating capacity were improved by 7.2% and 7.3%, respectively.

Keywords: High-temperature heat pump, two-phase ejector, mixing pressure, low–global warming potential refrigerants

1. Introduction

A high-temperature heat pump (HTHP) is one of the emerging solutions for decarbonization and electrification in industry and buildings. Current research focuses on HTHPs operating with electrically driven, single-stage vapor refrigerant compression cycles (VRCCs) [1]. A VRCC uses an expansion valve (EV) to reduce refrigerant pressure from the condenser to the evaporator, which is a throttling process associated with high energy loss. Using a two-phase ejector as an expander device to replace the EV could partially recover this energy loss, resulting in improved performance of the VRCC. A typical configuration of an HTHP operating with an ejector-expansion VRCC (EERC) is shown in Fig. 1(a). The configuration consists of a compressor, a condenser, an internal heat exchanger (IHX), a two-phase ejector, a separator, an evaporator, and an EV. Figure 1(b) shows that the ejector provides an isentropic expansion process (i.e., process 4→5), resulting in a larger specific enthalpy decrease than that associated with an isenthalpic expansion in an EV (i.e., process 4'→5'). Additionally, the ejector works as a thermo-compressor, providing a higher suction pressure for the compressor (i.e., $p_1 > p_1'$). An EERC could improve the performance of HTHPs by increasing the specific heat absorption capacity in the evaporator and reducing the compression work in the compressor [2].

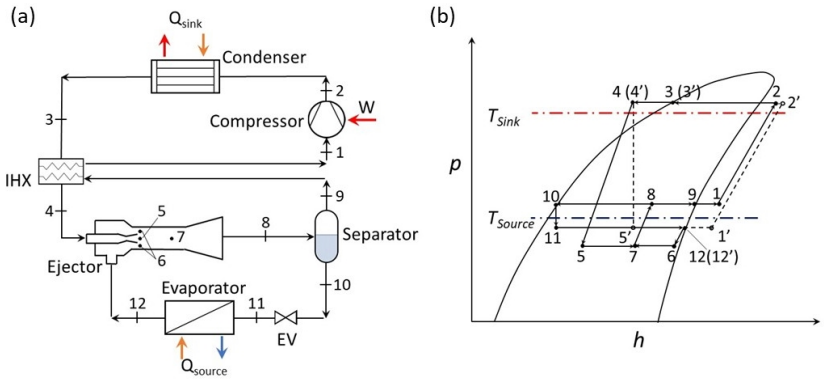

Fig. 1. HTHP assisted with a two-phase ejector: (a) configuration and (b) pressure-enthalpy diagram.

Using a two-phase ejector as an expander in EERCs was proposed in the 1930s. It became an exponentially increased research topic in HVAC and refrigeration (HVAC&R) systems in the 2010s [2, 3]. Two-phase ejectors have been employed in EERCs of transcritical CO_2 [4, 5] and subcritical, low-pressure refrigerants, such as R134a [6], R718 [7], R600a [8], R290 [9], and R410a [10]. For transcritical CO_2 EERCs with a high throttling loss, two-phase ejectors are attractive, increasing the cooling cycle coefficient of performance (COP) by 15%–30% [3]. For low-pressure refrigerant EERCs with a low throttling loss, a two-phase ejector is less effective, increasing the cooling cycle COP by 7%–20% [11]. The research on EERCs in HTHPs is limited. Popovac et al. [12] experimentally quantified the improved performance of an HTHP operating with R600 EERC and suggested that a two-phase ejector could improve the heating cycle COP by approximately 30% at a moderate temperature level (T_{sink} = 80.4°C and T_{source} = 53.2°C). Bai et al. [13] theoretically assessed EERCs operating with low–global warming potential (GWP) refrigerants and demonstrated that an EERC of R1234ze(Z) could improve the heating cycle COP by at least 10.3% at T_{sink} = 105°C and T_{source} = 30°C. Luo and Zou [14] theoretically showed that HTHPs with EERCs of R600 and R1234ze(Z) could reduce expansion losses by 10%–18% and improve the heating cycle COP by 8%–14% at T_{sink} = 120°C and T_{source} = 80°C. Mateu-Royo et al. [15] theoretically demonstrated that an EERC could slightly improve the heating cycle COP and downsize the compressor.

The majority of theoretical research has employed the zero-dimensional model developed by Kornhauser [16]. Kornhauser's model assumed the mixing process was under constant pressure, p_M, and the two-phase fluid was inhomogeneous at equilibrium. The model was built considering the conservation of mass, energy, and momentum with assigned efficiency for different sections within a two-phase ejector. The model required a specified p_M as an input to predict the component-level performance of two-phase ejectors. Pressure p_M is closely related to the ejector's geometry, refrigerants, and operating conditions, which are difficult to determine experimentally [2]. For a mixing process within a constant area under a constant pressure, p_M could be iteratively calculated from the relationship between the mass, flow area, and specific volumes of refrigerant [17-19]. However, the calculated p_M was affected by the condensation shock wave and/or the nonequilibrium two-phase flow at the exit of the mixing chamber. In other literature, p_M was guessed without justification. In transcritical CO_2 EERC for low-temperature refrigeration, $p_{M,opt}$ was assumed to be the evaporation pressure of secondary fluid (SF), p_{Evap}, by Deng et al. [20], or 95% of p_{Evap} by Purjam et al. [21]. In EERC using R134a, R1234yf, and R1234ze(Z) for refrigeration, p_{Evap} was assumed to be the saturated vapor pressure corresponding to a 5 K drop in the evaporation temperature, T_{evap}, by Lawrence and Elbel [22] and Atmaca et al. [23]. Additionally, Kornhauser's primary results showed that the maximum cooling cycle COP of EERC in refrigeration was achieved with an optimum mixing pressure, $p_{M,out}$, which gave the same velocity of the primary fluid (PF) and the SF before mixing. No evidence existed that the calculated or guessed p_M was $p_{M,out}$, which could yield the maximum COP of the investigated EERC for refrigeration applications.

To fully explore the technical merit of using a two-phase ejector in an HTHP, selecting a reasonable value of $p_{M,out}$ is critical. This study analyzes the optimized mixing pressure of two-phase ejectors in HTHPs. An improved 1D thermodynamic model of a two-phase ejector was built with the real properties of refrigerants. The effects of mixing pressure on fluid dynamics within two-phase ejectors were investigated. The optimum mixing pressure was determined for the component-level performance of two-phase ejectors and the system-

level performance of HTHPs. The technical merits of HTHPs with EERCs were explored for various low-GWP refrigerants.

2. Theoretical Model of a Two-Phase Ejector

A typical ejector consists of a primary nozzle, a suction chamber, a mixing chamber (including a converging section and a constant area section), and a diffuser, as shown in Fig. 2. The ejector works on the isentropic conversion process of potential work, contained in the PF flow, into kinetic energy. High-pressure PF accelerates into a high-speed jet and creates a low-pressure zone at the nozzle exit plane, which entrains the low-pressure SF vapor into the suction chamber. Depending on the initial state of the PF, the PF flow at the nozzle's exit could be supersonic (e.g., in transcritical CO_2 cycles [24]) or subsonic associated with two-phase change (e.g., flashing evaporation or condensation). PF flow further accelerates and expands, creating a hypothetical throat at the section *y-y*, where the SF flow may be choked at its critical velocity. PF and SF mix in the constant area section of the mixing chamber under a constant mixing pressure, p_M. If the flow of completely mixed PF and SF is supersonic, a condensation shock wave occurs, resulting in a pressure lift. The static pressure of mixed PF and SF further increases in the diffuser by converting its kinetic energy into potential energy.

2.1. Governing Equations

In this study, an improved 1D thermodynamic model of a two-phase ejector was built, considering a constant pressure mixing process [16, 25]. Major assumptions adopted in the theoretical model include the following:

(1) The flow inside the ejector is 1D, steady, and adiabatic.

(2) The frictional and mixing losses are defined in terms of ejector component isentropic efficiencies, including η_N for the primary nozzle, η_S for the secondary flow, η_M for the mixing process, and η_D for the diffuser [26].

(3) Working fluid is in thermodynamic quasi-equilibrium condition (i.e., a homogeneous equilibrium model of two-phase flow [27]).

(4) The mixing PF and SF is initiated at the section *y-y* and completed at the section *m-m* under constant static pressure, p_M.

The governing equations in the thermodynamic model are built with the mass, momentum, and energy conservation across the ejector components. The state points of fluids in the following equations are presented by lowercase Roman numerals "i, ii, iii, …", as shown in Fig. 2

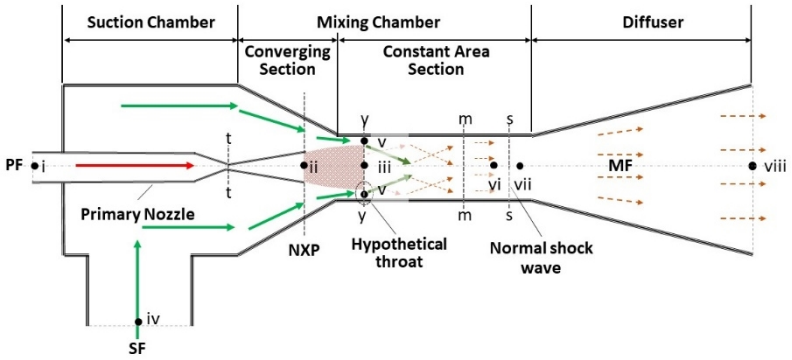

Fig. 2. Typical flow phenomena in a two-phase ejector [28]. (NXP stands for nozzle exit plane. MF represents the mixed PF and SF.)

The energy conservation of PF through an isentropic expansion process within the primary nozzle and the converging section of the mixing chamber is given by Eqs. (1) and (2):

$$h_{\mathrm{iii}} = (1-\eta_{\mathrm{N}})h_{\mathrm{i}} + \eta_{\mathrm{N}}h_{\mathrm{iii,is}}\text{ , and} \tag{1}$$

$$V_{\mathrm{iii}} = \sqrt{2(h_{\mathrm{i}} - h_{\mathrm{iii}})}. \tag{2}$$

The energy conservation of SF within the converging section of the mixing chamber is calculated with Eqs. (3) and (4):

$$h_{\mathrm{v}} = (1-\eta_{\mathrm{S}})h_{\mathrm{iv}} + \eta_{\mathrm{S}}h_{\mathrm{v,is}} \text{ and } h_{\mathrm{v,is}} = h(s_{\mathrm{iv}},p_{\mathrm{v}}), \text{ and} \tag{3}$$

$$V_{\mathrm{v}} = \sqrt{2(h_{\mathrm{vi}} - h_{\mathrm{v}})}. \tag{4}$$

The maximum value of V_{v} is limited to its local speed of sound, C_{v}. If the flow of SF is chocked, then Eq. (5) gives

$$V_{\mathrm{v,max}} = C_{\mathrm{v}}. \tag{5}$$

The mixing process is under constant static pressure, represented by Eq. (6):

$$p_{\mathrm{iii}} = p_{\mathrm{v}} = p_{\mathrm{vi}} = p_{\mathrm{M}}. \tag{6}$$

The moment conservation in the mixing process is given by Eq. (7):

$$\phi_{\mathrm{M}}(\dot{m}_{\mathrm{PF}}V_{\mathrm{iii}} + \dot{m}_{\mathrm{SF}}V_{\mathrm{v}}) = (\dot{m}_{\mathrm{PF}} + \dot{m}_{\mathrm{SF}})V_{\mathrm{vi}}, \tag{7}$$

where ϕ_{M} is the velocity coefficient accounting for the frictional loss in the mixing process, and $\phi_{\mathrm{M}} = \sqrt{\eta_{\mathrm{M}}}$ [29].

The energy conservation in the mixing process is shown in Eq. (8):

$$(\dot{m}_{\mathrm{PF}} + \dot{m}_{\mathrm{SF}})\left(h_{\mathrm{vi}} + \frac{1}{2}V_{\mathrm{vi}}^2\right) = \dot{m}_{\mathrm{PF}}\left(h_{\mathrm{iii}} + \frac{1}{2}V_{\mathrm{iii}}^2\right) + \dot{m}_{\mathrm{SF}}\left(h_{\mathrm{v}} + \frac{1}{2}V_{\mathrm{v}}^2\right). \tag{8}$$

If the mixed flow is supersonic or sonic (i.e., $M_{\mathrm{vi}} \geq 1$), a condensation shock will occur at the section s-s. The conservation of mass, momentum, and energy across a condensation shock wave are calculated by Eqs. (9), (10), and (11) [25]:

$$\rho_{\mathrm{vii}}V_{\mathrm{vii}} = \rho_{\mathrm{vi}}V_{\mathrm{vi}}, \tag{9}$$

$$p_{\mathrm{vii}} + \rho_{\mathrm{vii}}V_{\mathrm{vii}}^2 = p_{\mathrm{vi}} + \rho_{\mathrm{vi}}V_{\mathrm{vi}}^2, \text{ and} \tag{10}$$

$$h_{\mathrm{vii}} + \frac{1}{2}V_{\mathrm{vii}}^2 = h_{\mathrm{vi}} + \frac{1}{2}V_{\mathrm{vi}}^2. \tag{11}$$

The thermodynamic state equations for the density and entropy after the condensation shock wave are given in Eqs. (12) and (13):

$$\rho_{\mathrm{vii}} = \mathrm{rho}(p_{\mathrm{vii}},h_{\mathrm{vii}}), \text{ and} \tag{12}$$

$$s_{\mathrm{vii}} = s(p_{\mathrm{vii}},h_{\mathrm{vii}}). \tag{13}$$

If the mixed flow is subsonic (i.e., $M_{\mathrm{vi}} < 1$), Eq. (14) applies:

$$\mathrm{V}_{\mathrm{vii}} = V_{\mathrm{vi}}, p_{\mathrm{vii}} = p_{\mathrm{vi}}, \text{ and } s_{\mathrm{vii}} = s_{\mathrm{vi}} = s(p_{\mathrm{vi}},h_{\mathrm{vi}}) \tag{14}$$

The energy conservation within the diffuser is given by Eqs. (15) and (16):

$$h_{\mathrm{viii}} = h_{\mathrm{vii}} + \frac{1}{2}V_{\mathrm{vii}}^2, \text{ and} \tag{15}$$

$$h_{\mathrm{viii,is}} = h_{\mathrm{vii}} + \eta_{\mathrm{D}}\frac{1}{2}V_{\mathrm{vii}}^2. \tag{16}$$

The static pressure and quality of the two-phase fluid discharged from the ejector are given in Eqs. (17) and (18):

$$p_{\mathrm{viii}} = p(h_{\mathrm{viii,is}}, s_{\mathrm{viii}}) \text{ and } s_{\mathrm{viii}} = s_{\mathrm{vii}}, \text{ and} \tag{17}$$

$$x_{\mathrm{viii}} = x(p_{\mathrm{viii}}, h_{\mathrm{viii}}). \tag{18}$$

Assuming the discharged two-phase fluid could be fully separated in the separator, the fluid loop in an EERC requires Eq. (19):

$$x_{\mathrm{viii}} = \frac{\dot{m}_{\mathrm{PF}}}{\dot{m}_{\mathrm{PF}} + \dot{m}_{\mathrm{SF}}} = \frac{1}{1+\omega}, \tag{19}$$

where ω is the ratio of the mass flow rates of SF, $\dot{m}_{\mathrm{SF}}$, and to that of PF, $\dot{m}_{\mathrm{PF}}$, as shown in Eq. (20):

$$\omega = \frac{\dot{m}_{\mathrm{SF}}}{\dot{m}_{\mathrm{PF}}}. \tag{20}$$

The flow conditions in the ejector are characterized by the Mach number, *M*, and *M* = *V*/*C*. The speed of sound of the two-phase flow, *C*, is given in Eq. (21) [21]:

$$C = \frac{1}{(1-\alpha)\sqrt{\frac{1-\alpha}{c_{\mathrm{l}}^2} + \frac{\alpha\rho_{\mathrm{l}}}{\rho_{\mathrm{v}}c_{\mathrm{v}}^2}} + \alpha\sqrt{\frac{\alpha}{c_{\mathrm{v}}^2} + \frac{(1-\alpha)\rho_{\mathrm{v}}}{\rho_{\mathrm{l}}c_{\mathrm{l}}^2}}}, \tag{21}$$

where α is the void fraction of the two-phase flow, and ρ is the density. The subscripts l and v are for the saturated liquid and vapor phases of refrigerants. In a homogeneous two-phase flow, the void fraction is given by Eq. (22):

$$\alpha = \frac{x\rho_{\mathrm{l}}}{(x\rho_{\mathrm{l}} + (1-x)\rho_{\mathrm{v}})}, \tag{22}$$

where *x* is the vapor quality of the two-phase fluid.

2.2. Calculation Procedure

The two-phase ejector was operated with specified inlet temperature and static pressure of PF and SF, denoted as T_{i}, p_{i}, T_{iv}, and p_{iv}. In investigated ejector-assistant HTHPs, inlet PF was subcooled liquid, and inlet SF was saturated vapor.

$$\begin{aligned} T_{\mathrm{i}} &= T_{\mathrm{sink}} - \Delta T_{\mathrm{sc}} \quad p_{\mathrm{i}} = p(T_{\mathrm{sink}}, x = 1) \\ T_{\mathrm{iv}} &= T_{\mathrm{source}} = T_{\mathrm{sink}} - \Delta T_{\mathrm{lift}}, \end{aligned} \tag{23}$$

where T_{source} is the sink temperature, ΔT_{SC} is the subcooling temperature of PF from the IHX, and ΔT_{lift} is the lifted temperature of HTHPs. The mixing pressure, p_{M}, is the saturated vapor pressure of SF at an equivalent temperature of SF before mixing, T_{M}, given in Eq. (24):

$$T_{\mathrm{M}} = T_{\mathrm{Evap}} - \Delta T_{\mathrm{M}}, \tag{24}$$

where ΔT_{M} is the assumed temperature drop of saturated SF before the mixing process.

The calculation procedure for solving the two-phase ejector model is shown in Fig. 3. These governing equations were solved iteratively in the Engineering Equation Solver (EES, F-Chart software). Component efficiencies of two-phase ejectors were assumed with constant values: $\eta_{\mathrm{N}} = 0.8$, $\eta_{\mathrm{S}} = 0.8$, $\eta_{\mathrm{M}} = 0.9$, and $\eta_{\mathrm{D}} = 0.8$ [18]. For a specified p_{M}, the model could predict the pressure and quality of discharged two-phase fluid from the two-phase ejector, p_{viii} and x_{viii}.

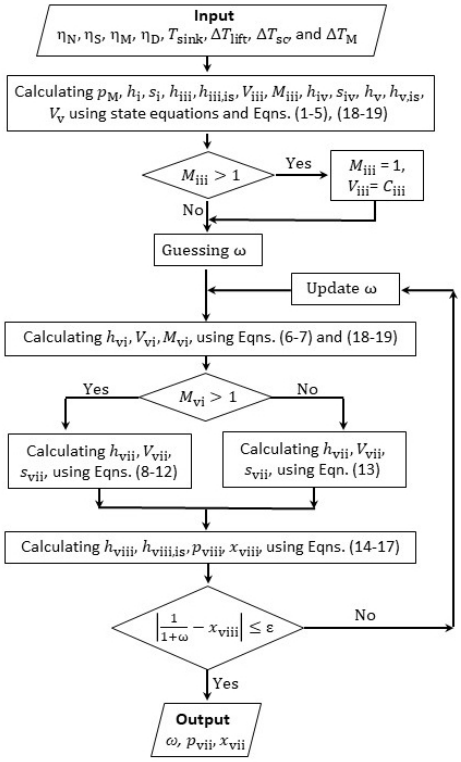

Fig. 3. Flow chart of solving the two-phase ejector model.

3. Thermodynamic Model of an Ejector-Assisted HTHP

A thermodynamic model of an HTHP with EERC was built by applying the mass and energy conservation within each component [15, 30], as summarized in Table 1. The theoretical model was solved using EES with its built-in thermophysical properties of the refrigerants. The system performance of HTHPs was evaluated with selected refrigerants under specified operating parameters of T_{sink}, ΔT_{lift}, and ΔT_{SC}. The system assumed the approach temperature and the pressure drops in the evaporator/condenser were negligible.

Table 1. Mass and energy equations in the thermodynamic model of an ejector-assisted HTHP

Component	Mass equations	Energy equations	Thermal properties equations
Compressor	$\dot{m}_2 = \dot{m}_1 = \dot{m}_{\text{PF}}$	$W_{\text{Comp}} = \frac{\dot{m}_1(h_{2,\text{is}} - h_1)}{\eta_{\text{is}}\eta_{\text{em}}}$	$h_{2,\text{is}} = h(p_2, s_2)$; $h_2 = h_1 + \eta_{\text{is}}(h_{2,\text{is}} - h_1)$; $p_2 = p_3$; $s_2 = s_1$
Condenser	$\dot{m}_3 = \dot{m}_2$	$Q_{\text{Sink}} = \dot{m}_3(h_2 - h_3)$	$h_3 = h(T_3, x = 0)$; $T_3 = T_{\text{sink}}$; $p_3 = p(T_3, x = 0)$
IHX	$\dot{m}_4 = \dot{m}_3 = \dot{m}_9 = \dot{m}_1$	$Q_{\text{IHX}} = \dot{m}_4(h_3 - h_4)$ $Q_{\text{IHX}} = \dot{m}_1(h_1 - h_9)$	$h_4 = h(T_4, p_4)$; $h_9 = h(p_9, x = 1)$; $p_4 = p_3$; $p_9 = p_8$; $T_4 = T_3 - \Delta T_{\text{sc}}$

Table 1. Mass and energy equations in the thermodynamic model of an ejector-assisted HTHP (continued)

Component	Mass equations	Energy equations	Thermal properties equations
Two-phase ejector	$\dot{m}_8 = \dot{m}_4 + \dot{m}_{12}$	$\dot{m}_8 h_8 = \dot{m}_4 h_4 + \dot{m}_{12} h_{12}$	$h_{12} = h(p_{12}, x = 1)$; p_8, x_8, and T_8 predicted form the ejector model

Separator	$\dot{m}_9 = \dot{m}_8 x_8$ $\dot{m}_{10} = \dot{m}_8(1 - x_8)$	$\dot{m}_9 h_9 + \dot{m}_{10} h_{10} = \dot{m}_8 h_8$	$h_9 = h(p_9, x = 1)$; $h_{10} = h(p_{10}, x = 0)$; $p_8 = p_9 = p_{10}$
Expansion valve	$\dot{m}_{11} = \dot{m}_{10}$	$\dot{m}_{11} h_{11} = \dot{m}_{10} h_{10}$	$h_{11} = h_{10}$
Evaporator	$\dot{m}_{12} = \dot{m}_{11} = \dot{m}_{SF}$	$Q_{Source} = \dot{m}_{12}(h_{12} - h_{11})$	$h_{12} = h(T_{12}, x = 1)$; $T_{12} = T_{source} = T_{sink} - \Delta T_{lift}$

3.1. Compressor

A piston compressor was used in the investigated HTHP for a heating capacity of ≤800 kW. The compressor could provide the maximum discharged temperature of 150°C using hydrofluoroolefins (HFOs) [31]. The volumetric and isentropic efficiencies of piston compressors, represented as η_{vol} and η_{is}, were predicted using Pierre's correlations in Eqs. (25) and (26) [32, 33]:

$$\eta_{vol} = 1.04\left(1 + 0.15\frac{T_{suc} - 18}{100}\right) \cdot \exp\left(-0.07\,\frac{p_{disch}}{p_{suc}}\right), \text{ and} \tag{25}$$

$$\left(\frac{\eta_{vol}}{\eta_{is}}\right) = \left(1 - 0.1\frac{T_{suc} - 18}{100}\right) \cdot \exp\left(-2.40\,\frac{T_{disch} + 273.15}{T_{suc} + 273.15} + 2.88\right), \tag{26}$$

where T_{suc} and T_{disch} are refrigerant temperatures in degrees Celsius, and p_{suc}, and p_{disch} are pressures at the compressor's inlet and outlet, denoted by state points 1 and 2 in Fig. 1(b), respectively.

The power consumption of the compress, W_{Comp}, is calculated by Eq. (27):

$$W_{Comp} = \frac{\dot{m}_{PF}(h_{2,is} - h_1)}{\eta_{is}\eta_{em}}, \tag{27}$$

where $h_{2,is}$ is the enthalpy of discharged refrigerant after an isentropic compression process, and η_{em} is the electromechanical efficiencies of compressor; $\eta_{em} = 0.95$.

3.2. *Internal Heat Exchanger*

An IHX is employed in HTHPs to ensure a dry compression process in the compressor and improve the COP of HTHPs [34]. An IHX exchanges the heat between high-pressure vapor and low-pressure liquid. Refrigerant vapor entering the IHX is saturated at the discharged pressure of the ejector. The enthalpy of superheated vapor leaving the IHX is determined from the energy balance between the liquid and vapor refrigerant in the IHX. In this study, the subcooling temperature of refrigerant leaving the IHX, ΔT_{SC}, was specified as an input in the theoretical model of the two-phase ejector, which should be large enough to ensure the superheating of vapor at the compressor outlet.

3.3. Two-Phase Ejector

The component-level performance of the ejector was evaluated by the entrainment ratio, ω, defined in Eq. (20), and the pressure lift ratio, Π, which is defined in Eq. (28) as the ratio of the ejector's discharged pressure, p_{viii}, to the inlet pressure of SF, p_{iv}:

$$\Pi = \frac{p_{EJT,out}}{p_{SF,in}} = \frac{p_{viii}}{p_{iv}} = \frac{p_8}{p_{12}}. \tag{28}$$

Elbel and Hrnjak [35] proposed the ejector efficiency, η_{EJT} as an appliable efficiency metric to evaluate the trade-off between ω and Π. η_{EJT} is the ratio of the actual amount of work recovered by the ejector, W_r, and the total work recovery potential for an isentropic process, $W_{r,max}$, given by Eq. (29):

$$\eta_{EJT} = \frac{W_r}{W_{r,max}\frac{h_A - h_B}{h_C - h_D}}, \tag{29}$$

where h_A and h_B are the enthalpy of the PF at the ejector's discharged pressure via isenthalpic and isentropic expansion processes, respectively. The entropy of SF flow before and after an isentropic compression process are h_C and h_D, respectively. For the investigated ejector-assisted HTHP in this study,

$$h_A = h_4, \qquad h_B = h(p = p_8, s = s_4),$$
$$h_C = h(p = p_8, s = s_{12}),$$
$$h_D = h_{12}. \tag{30}$$

3.4. Performance of Ejector-Assisted HTHPs

The system-level performance of ejector-assisted HTHPs is evaluated by its heating cycle COP, given in Eq. (31):

$$COP_{\mathrm{EHTHP}} = \frac{Q_{\mathrm{Sink}}}{W_{\mathrm{Comp}}}. \tag{31}$$

The refrigerants for the ejector-assisted HTHPs were evaluated by the volumetric heating capacity (VHC) [36]. A higher value of VHC is desired for a smaller compressor displacement rate to deliver a specified capacity, as shown in Eq. (32):

$$VHC = \eta_{\mathrm{vol}} \rho_1 (h_2 - h_3). \tag{32}$$

3.5. Low-GWP Refrigerants

Low-GWP refrigerants promising for HTHPs were selected to evaluate the merit of ejector-assisted HTHPs, as listed in Table 2. These refrigerants can be categorized into hydrocarbon (HC), hydrochlorofluorocarbon (HCFO), and HFO. R245fa is R-245fa is a hydrofluorocarbon (HFC) and set as a reference refrigerant because of its wide use in current HTHPs.

Table 2. Low-GWP refrigerants for ejector-assisted HTHPs

Group	Refrigerants	Formula	T_{cr} [°C]	P_{cr} [MPa]	ρ_v* [kg/m³]	*NBP*** [°C]	*MW*** [kg/kmol]	ODP**	GWP	SC***
HC	R601	C_5H_{12}	196.6	3.37	10.1	36.1	72.2	0	5	A3
	R600	C_4H_{10}	152.0	3.80	25.2	−0.5	58.1	0	4	A3
HCFO	R1233zd(E)	$C_3ClF_3H_2$	166.5	3.62	34.8	18.3	130.5	0.00034	1	A1
	R1224yd(Z)	C_3ClF_4H	155.5	3.33	45.6	14.6	148.5	0.00012	<1	A1
HFO	R1336mzz(Z)	$C_4F_6H_2$	171.4	2.90	27.5	33.4	164.1	0	2	A1
	R1234ze(Z)	$C_3F_4H_2$	150.1	3.53	42.2	9.8	114.0	0	<1	A2L
HFC	R245fa	$C_3F_5H_3$	154.0	3.65	44.1	15.1	134.0	0	858	B1

*Saturated vapor at 80.0°C.
**NBP is normal boiling point. MW is molecular weight. ODP is ozone depletion potential.
***ASHRAE safety class (SC): A and B for toxicity from low to high, 1, 2L, 2, and 3 for flammability from low to high.

4. Results and Discussion

The ejector-assisted HTHPs were operated at T_{sink} = 120°C, ΔT_{lift} = 40 K, and ΔT_{SC} = 10 K. The component isentropic efficiencies of a two-phase ejector were η_N = 0.8, η_S = 0.8, η_M = 0.9, and η_D = 0.8. The effects of the mixing pressure, p_M, on the component-level performance of a two-phase ejector was predicted by the theoretical model with various equivalent temperature drops of SF (i.e., ΔT_M in Eq. (25)). For R1336mzz(Z), p_M in the two-phase ejector almost linearly decreased from 429.2 kPa to 235.0 kPa as ΔT_M increased from 0.1 K to 21.4 K.

4.1. Effects of the Mixing Pressure

4.1.1. Component-level performance of two-phase ejector

With the decrease of p_M, the velocity of PF and SF flows increased, and the velocity of SF flow increased more significantly than that of PF flow, as shown in Fig. 4(a). This difference is because the enthalpy change of SF (saturated vapor) is much larger than that of PF (low-quality two-phase fluid) through an isentropic expansion process across the same pressure drop. The *p-h* diagram of R1336mzz(Z) shows that the isenthalpic and isentropic lines are nearly parallel in the low-quality two-phase region, and the slopes of isenthalpic lines are much smaller than those of isentropic lines in the high-quality two-phase region. With the decrease of p_M, the discharged pressure of ejector, p_{viii}, increased to the maximum value of 456 kPa, giving the maximum pressure lift ratio, Π_{max}. After that maximum, p_{viii} linearly decreased.

From the velocity and the static pressure of PF and SF before the mixing process, four unique points could be identified as: the maximum pressure lift ratio, Π_{max}; no pressure lift effect, $\Pi = 1$; the same velocity of PF and SF, $V_{SF} = V_{PF}$; and a choked SF flow, $M_{SF} = 1$. The effects of p_M on the component performance of two-phase ejectors are shown in Fig. 5. The trends of ω and η_{EJT} related to p_M are similar to that of Π. At the optimum mixing pressure, $p_{M,opt}$ = 424.7 kPa with ΔT_M = 0.6 K, the maximum values of ω_{max} = 0.733, Π_{max} = 1.059, and $\eta_{EJT,max}$ = 0.333 were achieved. At p_M = 358.2 kPa (with ΔT_M = 6.8 K), Π = 1 and η_{EJT} = 0. Further reducing p_M, the ejector could not provide a compression effect because of the overexpansion of PF in the primary nozzle. At p_M = 349.4 kPa (with ΔT_M = 7.7 K), $V_{SF} = V_{PF}$, $\Pi < 1$, and $\eta_{EJT} < 0$. These values indicate that selecting p_M for $V_{SF} = V_{PF}$ is not beneficial for the performance of two-phase ejectors. When p_M was reduced to 235 kPa (with ΔT_M =21.4 K), p_M was sufficiently low to accelerate the SF flow to M_{SF} = 1, and the PF flow was subsonic, with M_{PF} =0.77. At this p_M, the mixed PF and SF flow at the section *m-m* was subsonic; thus, a condensation shock wave did not occur [37]. Further reducing p_M may accelerate the PF flow to supersonic, but the performance of the two-phase ejector would extremely deteriorate.

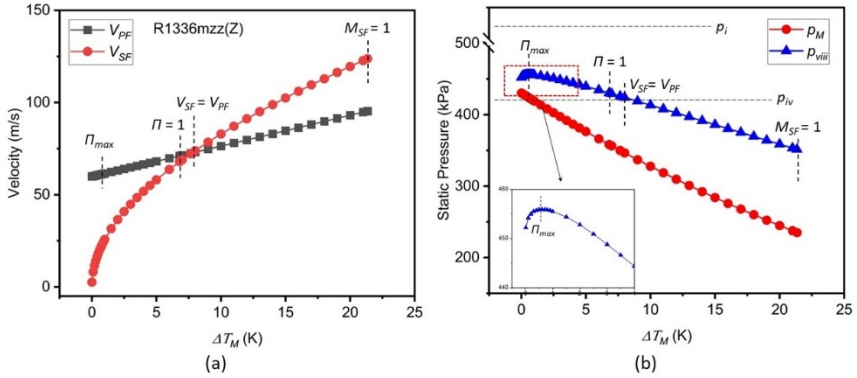

Fig. 4. Effects of the mixing pressure on the gas dynamic properties in a two-phase ejector: (a) velocity and (b) static pressure.

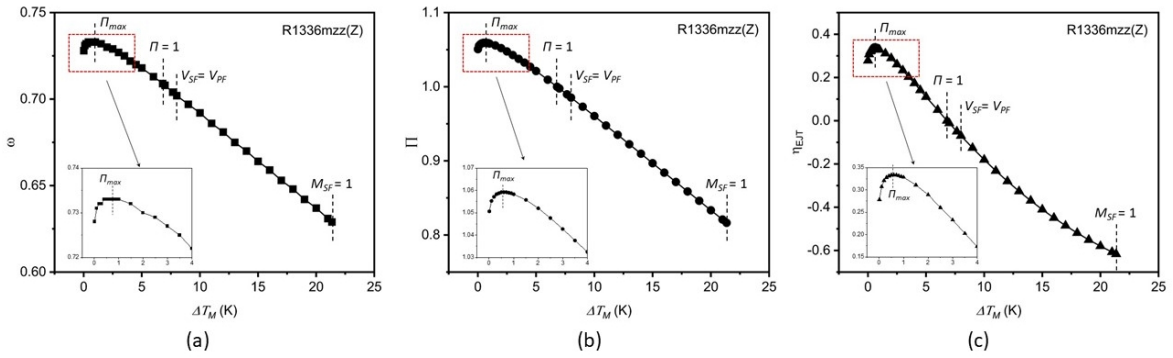

Fig. 5. Effects of the mixing pressure on the two-phase ejector's performance: (a) entrainment ratio, (b) pressure lift ratio, and (c) ejector efficiency.

4.1.2. System-level performance of ejector-assisted HTHPs

The system-level performance of an ejector-assisted HTHP is closely related to the component-level performance of a two-phase ejector. The maximum values of COP and VHC were achieved with $\eta_{EJT,max}$ at $p_{M,opt}$, as shown in Fig. 6. The reference values of COP and VHC, represented as COP_{ref} and VHC_{ref}, are for HTHPs with an EV. COP_{max} = 6.29 and VHC_{max} = 3,272 kJ/m^3 were achieved at $p_{M,opt}$, corresponding to the improvement of ΔCOP_{max} = 7.01% and ΔVHC_{max} = 7.63% for R1336mzz(Z). Replacing an EV with a two-phase ejector becomes unfavorable in HTHPs when the ejector cannot provide the compression effect (i.e., $\Pi \leq 1$).

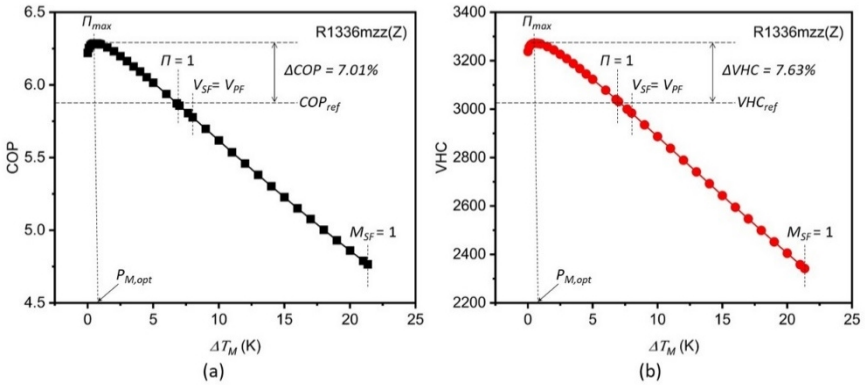

Fig. 6. Effects of the mixing pressure on the performance of an ejector-assisted HTHP: (a) COP and (b) VHC.

4.2. Effects of the Refrigerants

The performance of two-phase ejectors and ejector-assisted HTHPs with selected refrigerants under specified operating conditions (i.e., T_{sink} = 120°C, ΔT_{lift} = 40 K, and ΔT_{SC} = 10 K), as shown in Fig. 7. Similar to R1366mzz(Z), the mixing pressure had an optimum value for the maximum values of η_{EJT}, COP, and VHC, as summarized in Table 3. The averaged value of η_{EJT} was 0.334 ± 0.005, improving the performance of HTHPs by ΔCOP = 7.2% ± 0.9% and ΔVHC = 7.3% ± 0.7%. This work demonstrates that replacing an EV with a two-phase ejector improves the COP of HTHPs and requires more compact compressors than basic HTHPs, which is consistent with previous studies [11]. The contribution of the two-phase ejector in the COP improvement of HTHPs with low-GWP refrigerant is 5.79%–8.47%, which is much lower than moderate-temperature HPs with transcritical CO_2 (ΔCOP = 15%–30% [3]). Compared with R245fa, two-phase ejectors contribute to lower improvements of COP and VHC with the selected low-GWP refrigerants, except for the improved COP with R600. R600 presented the highest COP improvement of 8.47% and the highest VHC values of 6,090 kJ/m^3.

For HTHPs under specified operating conditions, $p_{M,opt}$ was approximately 98.4% ± 0.2% of p_{Evap}, which was slightly larger than 95% of p_{Evap} for a transcortical CO_2 EERC refrigeration system [21]. ΔT_M for $p_{M,opt}$ was 0.7°C ± 0.1°C, which was much smaller than ΔT_M = 5 K for EERC refrigeration using R134a, R1234yf, and R1234ze(E) [22, 23]. A higher value of $p_{M,opt}/p_{Evap}$, associated with a lower ΔT_M, for two-phase ejectors in HTHPs may be because of the high operating temperature of low-pressure refrigerants and the ejector components' isentropic efficiencies adopted in the theoretical model. Additionally, this study demonstrated that p_M for $V_{SF} = V_{PF}$ does not give the maximum COP of ejector-assisted HTHPs. This result disagrees with Kornhauser's primary analysis, which claimed that $p_{M,opt}$ was for $V_{SF} = V_{PF}$ [16]. In a supersonic ejector, the same velocities of PF and SF in the mixing process theoretically results in minimal kinetic energy loss associated with the velocity difference [38]. However, this effect may not be significant in a two-phase ejector because of the subsonic flow combined with a two-phase transition process.

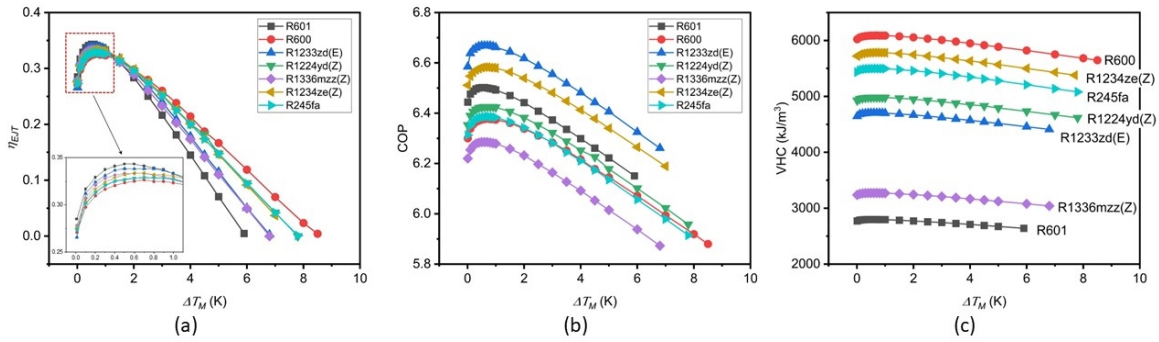

Fig. 7. Ejector-assisted HTHPs with different refrigerants: (a) ejector efficiency, (b) COP, and (c) VHC.

Table 3. Performance of an ejector-assisted HTHP with different refrigerants

Refrigerants	Two-phase ejector			Ejector-assisted HTHP		Maximum improvement	
	ΔT_M (K)	p_M/p_{Evap} (%)	η_{EJT}	COP	VHC (kJ/m^3)	ΔCOP (%)	ΔVHC (%)
R601	0.6	98.5	0.343	6.50	2,798	5.79	6.07
R600	0.7	98.5	0.327	6.38	6,090	8.47	7.85
R1233zd(E)	0.5	98.8	0.339	6.67	4,703	6.5	6.62
R1224yd(Z)	0.8	98.1	0.329	6.43	4,982	7.84	7.91
R1336mzz(Z)	0.6	98.2	0.333	6.29	3,272	7.02	7.63
R1234ze(Z)	0.7	98.3	0.334	6.58	5,784	7.28	7.47
R245fa	0.7	98.2	0.330	6.39	5,499	8.02	8.27

5. Conclusions

The ejector-assisted HTHP used a two-phase ejector to replace an EV, improving energy efficiency and reducing the compressor size. These improvements closely relate to the component-level performance of two-phase ejectors. This study investigated the effects of mixing pressure on the component-level performance of two-phase ejectors and the system-level performance of ejector-assisted HTHPs. A 1D theoretical model was built to predict the fluid dynamic properties of refrigerants within the two-phase ejector and evaluate the ejector's performance. A thermodynamic model of ejector-assisted HTHP was built to evaluate the COP and VHC of HTHPs. Low-GWP refrigerants were selected for the ejector-assisted HTHPs. The effects of the mixing pressure on the component-level performance of two-phase ejectors and the system-level performance of ejector-assisted HTHPs were investigated under specified operating conditions: T_{sink} = 120°C, ΔT_{lift} = 40 K, and ΔT_{SC} = 10 K. The main conclusions are as follows:

(1) An optimum mixing pressure exists in a two-phase ejector, which gives the maximum performance of the two-phase ejector and ejector-assisted HTHP under specified working conditions.
(2) The optimum mixing pressure in a two-phase ejector for HTHPs is slightly lower than the evaporation pressure of SF.
(3) At the optimum mixing pressure, the two-phase flow in a two-phase ejector is subsonic. Choked flow and condensation shock waves do not occur.
(4) A two-phase ejector improves the performance of HTHPs with low-GWP refrigerants. But, the improvement of COP is less than that of transcritical CO_2 HTHPs.

Some limitations of this primary study need to be addressed in future studies. The developed 1D theoretical model of a two-phase ejector adopted constant values for the ejector component isentropic efficiencies. Particularly, the energy loss owing to the difference in the velocity of PF and SF was not considered in the isentropic efficiency of mixing process. These isentropic efficiencies are closely related to the working fluids, the ejector's geometry, and operating conditions. Computational fluid dynamics analysis needs to be employed to determine these isentropic efficiencies. This study provided a comprehensive analysis of the optimum

mixing pressure for ejector-assisted HTHPs operated with specified parameters. The effects of HTHPs operating parameters on the merits of two-phase ejectors needs to be investigated.

Acknowledgments

This work was sponsored by the US Department of Energy's Building Technologies Office under contract No. DE-AC05-00OR22725 with UT-Battelle, LLC. The authors would like to acknowledge the technology manager, Mr. Antonio Bouza, for his support.

NOMENCLATURE

Abbreviations

COP	coefficient of performance
EERC	ejector-assistant vapor compression
EV	expansion valve
GWP	global warming potential
HC	hydrocarbon
HCFO	hydrochlorofluorocarbon
HFC	hydrofluorocarbon
HFO	hydrofluoroolefin
HTHP	high-temperature heat pump
IHX	internal heat exchanger
MW	molecular weight (kg/kmol)
NBP	normal boiling point (°C)
ODP	ozone depletion potential
PF	primary fluid
SC	safety class
SF	secondary fluid
VHC	vapor heating capacity (kJ/m^3)
VRCC	vapor refrigerant compression cycle

Variables

C	speed of sound (m/s)
h	enthalpy of working fluids (kJ/kg)
$\dot{m}$	mass flow rate (kg/s)
M	Mach number
T	temperature (°C)
Q	thermal capacity (kW)
W	power (kJ/kg)
V	velocity (m/s)
x	quality of vapor
ρ	density (kg/m^3)
α	void fraction of two-phase flow
η	component efficiency
Π	pressure lift ratio in ejector
ϕ	velocity coefficient in ejectors
ω	entrainment ratio

Subscripts

1, 2, 3,…	state points within the loop of ejector heat pumps
lv	latent heat of evaporation
D	diffuser
disch	discharged vapor from the compressor

M	mixing chamber
max	maximum
N	primary nozzle of ejector
i, ii, iii, …	state points within an ejector
r	recovery
opt	optimum
S	suction chamber
SC	supercooling
suc	suction vapor into the compressor

References

[1] C. Arpagaus, F. Bless, M. Uhlmann, J. Schiffmann, and S. S. Bertsch, "High temperature heat pumps: Market overview, state of the art, research status, refrigerants, and application potentials," *Energy,* vol. 152, pp. 985-1010, 2018/06/01/ 2018, doi: https://doi.org/10.1016/j.energy.2018.03.166.

[2] S. Elbel, "Historical and present developments of ejector refrigeration systems with emphasis on transcritical carbon dioxide air-conditioning applications," *International Journal of Refrigeration,* vol. 34, no. 7, pp. 1545-1561, 2011/11/01/ 2011, doi: https://doi.org/10.1016/j.ijrefrig.2010.11.011.

[3] S. Elbel and N. Lawrence, "Review of recent developments in advanced ejector technology," *International Journal of Refrigeration,* vol. 62, pp. 1-18, 2016/02/01/ 2016, doi: https://doi.org/10.1016/j.ijrefrig.2015.10.031.

[4] M. Palacz, J. Bodys, M. Haida, J. Smolka, and A. J. Nowak, "Two-phase flow visualisation in the R744 vapour ejector for refrigeration systems," *Applied Thermal Engineering,* vol. 210, p. 118322, 2022.

[5] P. Gullo, M. R. Kærn, M. Haida, J. Smolka, and S. Elbel, "A review on current status of capacity control techniques for two-phase ejectors," *International Journal of Refrigeration,* vol. 119, pp. 64-79, 2020/11/01/ 2020, doi: https://doi.org/10.1016/j.ijrefrig.2020.07.014.

[6] K. Ameur, Z. Aidoun, and M. Ouzzane, "Experimental performances of a two-phase R134a ejector," *Experimental Thermal and Fluid Science,* vol. 97, pp. 12-20, 2018/10/01/ 2018, doi: https://doi.org/10.1016/j.expthermflusci.2018.03.034.

[7] M. N. Šarevski and V. N. Šarevski, "Characteristics of R718 refrigeration/heat pump systems with two-phase ejectors," *International Journal of Refrigeration,* vol. 70, pp. 13-32, 2016/10/01/ 2016, doi: https://doi.org/10.1016/j.ijrefrig.2016.07.007.

[8] Y. Jeon, S. Kim, D. Kim, H. J. Chung, and Y. Kim, "Performance characteristics of an R600a household refrigeration cycle with a modified two-phase ejector for various ejector geometries and operating conditions," *Applied Energy,* vol. 205, pp. 1059-1067, 2017.

[9] Y. Gao, G. He, D. Cai, and M. Fan, "Performance evaluation of a modified R290 dual-evaporator refrigeration cycle using two-phase ejector as expansion device," *Energy,* vol. 212, p. 118614, 2020/12/01/ 2020, doi: https://doi.org/10.1016/j.energy.2020.118614.

[10] Y. Jeon, J. Jung, D. Kim, S. Kim, and Y. Kim, "Effects of ejector geometries on performance of ejector-expansion R410A air conditioner considering cooling seasonal performance factor," *Applied Energy,* vol. 205, pp. 761-768, 2017.

[11] Z. Zhang, X. Feng, D. Tian, J. Yang, and L. Chang, "Progress in ejector-expansion vapor compression refrigeration and heat pump systems," *Energy Conversion and Management,* vol. 207, p. 112529, 2020/03/01/ 2020, doi: https://doi.org/10.1016/j.enconman.2020.112529.

[12] M. Popovac, M. Lauermann, A. Baumhakel, and G. Drexler-Schmid, "Performance analysis of a high-temperature heat pump with ejector based on butane as the refrigerant," in *12th IEA Heat Pump Conference, Vienna, Austria*, 2017.

[13] T. Bai, G. Yan, and J. Yu, "Thermodynamic assessment of a condenser outlet split ejector-based high temperature heat pump cycle using various low GWP refrigerants," *Energy,* vol. 179, pp. 850-862, 2019/07/15/ 2019, doi: https://doi.org/10.1016/j.energy.2019.04.191.

[14] B. Luo and P. Zou, "Performance analysis of different single stage advanced vapor compression cycles and refrigerants for high temperature heat pumps," *International Journal of Refrigeration,* vol. 104, pp. 246-258, 2019.

[15] C. Mateu-Royo, C. Arpagaus, A. Mota-Babiloni, J. Navarro-Esbrí, and S. S. Bertsch, "Advanced high temperature heat pump configurations using low GWP refrigerants for industrial waste heat recovery: A comprehensive study," *Energy Conversion and Management,* vol. 229, p. 113752, 2021/02/01/ 2021, doi: https://doi.org/10.1016/j.enconman.2020.113752.

[16] A. A. Kornhauser, "The use of an ejector as a refrigerant expander," presented at the International Refrigeration and Air Conditioning Conference, West Lafayette, IN, United States 1990, 82. [Online]. Available: https://docs.lib.purdue.edu/iracc/82/.

[17] D. Li and E. A. Groll, "Transcritical CO2 refrigeration cycle with ejector-expansion device," *International Journal of refrigeration,* vol. 28, no. 5, pp. 766-773, 2005.

[18] H. K. Ersoy and N. Bilir Sag, "Preliminary experimental results on the R134a refrigeration system using a two-phase ejector as an expander," *International Journal of Refrigeration,* vol. 43, pp. 97-110, 2014/07/01/ 2014, doi: https://doi.org/10.1016/j.ijrefrig.2014.04.006.

[19] J. Sarkar, "Optimization of ejector-expansion transcritical CO2 heat pump cycle," *Energy,* vol. 33, no. 9, pp. 1399-1406, 2008/09/01/ 2008, doi: https://doi.org/10.1016/j.energy.2008.04.007.

[20] J.-q. Deng, P.-x. Jiang, T. Lu, and W. Lu, "Particular characteristics of transcritical CO2 refrigeration cycle with an ejector," *Applied Thermal Engineering,* vol. 27, no. 2, pp. 381-388, 2007/02/01/ 2007, doi: https://doi.org/10.1016/j.applthermaleng.2006.07.016.

[21] M. Purjam, K. Thu, and T. Miyazaki, "Thermodynamic modeling of an improved transcritical carbon dioxide cycle with ejector: Aiming low-temperature refrigeration," *Applied Thermal Engineering,* vol. 188, p. 116531, 2021/04/01/ 2021, doi: https://doi.org/10.1016/j.applthermaleng.2020.116531.

[22] N. Lawrence and S. Elbel, "Experimental investigation of a two-phase ejector cycle suitable for use with low-pressure refrigerants R134a and R1234yf," *International Journal of Refrigeration,* vol. 38, pp. 310-322, 2014/02/01/ 2014, doi:

https://doi.org/10.1016/j.ijrefrig.2013.08.009.

[23] A. U. Atmaca, A. Erek, and O. Ekren, "Impact of the mixing theories on the performance of ejector expansion refrigeration cycles for environmentally-friendly refrigerants," *International Journal of Refrigeration,* vol. 97, pp. 211-225, 2019/01/01/ 2019, doi: https://doi.org/10.1016/j.ijrefrig.2018.09.013.

[24] Y. Zhu and P. Jiang, "Experimental and numerical investigation of the effect of shock wave characteristics on the ejector performance," *International Journal of Refrigeration,* vol. 40, pp. 31-42, 2014.

[25] Y. Liu, M. Yu, and J. Yu, "An improved 1-D thermodynamic modeling of small two-phase ejector for performance prediction and design," *Applied Thermal Engineering,* vol. 204, p. 118006, 2022/03/05/ 2022, doi: https://doi.org/10.1016/j.applthermaleng.2021.118006.

[26] F. Liu and E. A. Groll, "Study of ejector efficiencies in refrigeration cycles," *Applied Thermal Engineering,* vol. 52, no. 2, pp. 360-370, 2013/04/15/ 2013, doi: https://doi.org/10.1016/j.applthermaleng.2012.12.001.

[27] Ø. Wilhelmsen, A. Aasen, K. Banasiak, H. Herlyng, and A. Hafner, "One-dimensional mathematical modeling of two-phase ejectors: Extension to mixtures and mapping of the local exergy destruction," *Applied Thermal Engineering,* p. 119228, 2022.

[28] S. Elbel and P. Hrnjak, "Ejector refrigeration: an overview of historical and present developments with an emphasis on air-conditioning applications," presented at the International Refrigeration and Air Conditioning Conference, 2008, 884.

[29] B. Huang, J. Chang, C. Wang, and V. Petrenko, "A 1-D analysis of ejector performance," *International journal of refrigeration,* vol. 22, no. 5, pp. 354-364, 1999.

[30] A. Mota-Babiloni, C. Mateu-Royo, J. Navarro-Esbrí, F. Molés, M. Amat-Albuixech, and Á. Barragán-Cervera, "Optimisation of high-temperature heat pump cascades with internal heat exchangers using refrigerants with low global warming potential," *Energy,* vol. 165, pp. 1248-1258, 2018/12/15/ 2018, doi: https://doi.org/10.1016/j.energy.2018.09.188.

[31] M. Nilsson, H. N. Rislå, and K. Kontomaris, "Measured performance of a novel high temperature heat pump with HFO-1336mzz (Z) as the working fluid," in *12th IEA Heat Pump Conference*, 2017, pp. 14-17.

[32] E. Navarro-Peris, J. M. Corberán, L. Falco, and I. O. Martínez-Galván, "New non-dimensional performance parameters for the characterization of refrigeration compressors," *International Journal of Refrigeration,* vol. 36, no. 7, pp. 1951-1964, 2013/11/01/ 2013, doi: https://doi.org/10.1016/j.ijrefrig.2013.07.007.

[33] C. Mateu-Royo, J. Navarro-Esbrí, A. Mota-Babiloni, and Á. Barragán-Cervera, "Theoretical performance evaluation of ejector and economizer with parallel compression configurations in high temperature heat pumps," *International Journal of Refrigeration,* vol. 119, pp. 356-365, 2020.

[34] S. Elbel and P. S. Hrnjak, "EFFECT OF INTERNAL HEAT EXCHANGER ON PERFORMANCE OF TRANSCRITICAL C02 SYSTEMS WITH EJECTOR," 2004.

[35] S. Elbel and P. Hrnjak, "Experimental validation of a prototype ejector designed to reduce throttling losses encountered in transcritical R744 system operation," *International Journal of Refrigeration,* vol. 31, no. 3, pp. 411-422, 2008.

[36] D. Wu, B. Hu, R. Z. Wang, H. Fan, and R. Wang, "The performance comparison of high temperature heat pump among R718 and other refrigerants," *Renewable Energy,* vol. 154, pp. 715-722, 2020/07/01/ 2020, doi: https://doi.org/10.1016/j.renene.2020.03.034.

[37] F. Wang, D. Y. Li, and Y. Zhou, "Analysis for the ejector used as expansion valve in vapor compression refrigeration cycle," *Applied Thermal Engineering,* vol. 96, pp. 576-582, 2016/03/05/ 2016, doi: https://doi.org/10.1016/j.applthermaleng.2015.11.095.

[38] D. Buyadgie, O. Buyadgie, S. Artemenko, A. Chamchine, and O. Drakhnia, "Conceptual design of binary/multicomponent fluid ejector refrigeration systems," *International Journal of Low-Carbon Technologies,* vol. 7, no. 2, pp. 120-127, 2012.